PAPER #302

8º CONGRESSO PANAMERICANO DE INGENIERIA NAVAL,
TRANSPORTE MARÍTIMO E INGENIERIA PORTUARIA
1983

NUMERICAL SIMULATION OF THE LOW FREQUENCY MOTIONS AND MOORING LINE TENSIONS OF AN OFFSHORE MOORED VESSEL

Authors: CELSO P. PESCE, DANTON NUNES, GABRIEL F. GUELER, JOSÉ THOME DE CARVALHO FILHO.

ABSTRACTS

This work presents a time domain procedure for simulation of offshore mooring system behaviour, with emphasis on the slow-varying motions. General environmental conditions are considered as irregular waves, wind and current, no matter the heading angle. Non-linear characteristics of the mooring-system are preserved. Semi-empirical approachs are assumed, but exact models can be easily introduced. Examples are shown for a particular case.

RESUMO

Apresenta-se um modelo de simulação do comportamento de sistemas de amarração "offshore", com ênfase aos movimentos em baixa frequência.

Condições ambientais bastante gerais são consideradas tais como ondas irregulares, vento e corrente em quaisquer ângulos de aproamento. O procedimento apresentado preserva as características não lineares do sistema de amarração, e é construído a partir de modelo semi-empiricos. São apresentados exemplos de resultados de um caso particular de simulação.

1. INTRODUCTION

Ocean Research activities has been steadly stimulated as consequence of the offshore industry growth in recent years, raising new questions and solving engineering problems only slightly touched in the past.

Offshore mooring is a tipycal example of such problems. A mooring system fail can be responsible by human life, material and ecological losses.

Offshore moored tankers, crane-ships, pipelaying barges, semi-submersible platforms, drilling-ships, wave-breakers, are examples of oceanic systems that use mooring systems for positioning and operation.

Neverthless, a non-linear effect, known as slow-drift oscillations and not predicted by conventional first-order aproximation to the wave diffraction problem, assumes a great importance, difficulting a simplier treatment for the present study.

The exciting wave forces action, if considered to second-order, causes the system to move away from its static equilibrium position and to oscillate about such position in two distinct frequency ranges.

The first range corresponds to the wave spectrum one, the dynamical behaviour study being the conventional first-order seakeeping theory.

In the second range, the system oscillates slowly. The amplitudes of such motions may be of the same, or even higher, order of magnitude than first-order motions. Fig. 1 shows typical

mooring forces time series recorded in full scale at Curimã field

May authors have shown the ressonant nature of such behaviour, where the low eingen-frequencies of the mooring-vessel system are excited by second-order forces pulsing at wave group frequencies. Actually the frequency-structure of the second-order wave force spectrum are closely related to wave spectrum bandwidth by means of a quadratic amplitude demodulation.

Current and wind action can also excite slow-drift oscillations and its effects are also studied in the present paper in a semi-empirical way.

A dynamic simulation model in the low frequency range is here developed, accounting for wave, wind and current actions, no matter the heading angles. Such model is based on a semi-empirical approach and takes into account the non-linear characteristics of the mooring system.

2. DYNAMIC SIMULATION MODEL

The following basic assumptions are made:

- horizontal plane motions in a low frequency range
- no cross effects between horizontal plane motions and out-of-plane motions
- inertia of mooring system is negligeable
- drag on mooring system is not considered
- only anchor's chains are considered, neglecting elasticity
- strip theory applied for computation of dissipative forces
- potential flow is taken for wave train propagation.

Under such assumptions a time domain model was implemented to describe the dynamic of a moored vessel on the horizontal plane at very low frequencies.

Time domain simulation gives a good visualization of the dynamic behaviour of the system and allows to consider cases as intermediate buoys and events as chain rupture, or buoy submergence.

Exciting forces computations are based on semi-empirical models. Further models for wave exciting forces computation, including non-linear diffraction, will be easily introduced in the present model.

The time domain simulation procedure follows these steps:

for t_o to t_f do:

begin

- evaluate exciting forces due to environment;
- compute dissipative forces using strip method;
- for each mooring the
  compute restoring force from dimensionless curves;
  accumulate total restoring forces and moment;

- calculate the inertia force;
- integrate the equation of motion;
- propagate the irregular wave train using linear dispertion relationship;

end

The system's initial conditions are taken from preprocessed static equilibrium position.

2.1. Ship's Dynamic on the Horizontal Plane

On the horizontal plane two reference frames will be used in ship's motion simulation (see Fig. 2):

- o system $Oxy\psi$ - inertial frame
- o system $Guv\psi$ - fixed at the body, centered on C.G.

Denoting by B the transformation matrix from $Guv\psi$ to $Oxy\psi$ the equation of motion can be written, in the inertial frame:

$$BMB^{-1}\ddot{q} = \sum_i f_i \quad (1*) \qquad (2.1)$$

where:

M = inertia matrix defined in $Guv\psi$
q = $|x_G,\ y_G,\ \psi|^t$ (2*)
f_i = external exciting forces(wind, waves, current and mooring forces)

Considering longitudinal symetri, and no influences from out-of-plane motions (as roll) the inertia matrix can be written as:

$$M = \begin{vmatrix} 1 + a_{uu} & 0 & 0 \\ 0 & 1 + a_{vv} & r.a_{v\psi} \\ 0 & r.a_{\psi v} & r^2(1 + a_{\psi\psi}) \end{vmatrix} m \qquad (2.2)$$

(1*) dot denotes time derivative
(2*) $|\ |^t$ denotes transpose

where:

m = ship's mass

r = yaw radius of gyration

a_{ij} = added mass coefficients

Notice that attention is focused on slow varying motions on the horizontal plane and so the added mass coefficients must be known at very low frequencies.

Defining the state vector by $X^t = (q^t, \dot{q}^t)$, equation (1) is reduced to a first order differential equation:

$$\dot{X} = \begin{bmatrix} 0 & I_3 \\ 0 & 0 \end{bmatrix} X + \begin{bmatrix} 0 \\ Q \end{bmatrix} \tag{2.3}$$

where:

$Q = BM^{-1}B^{-1} \sum_i f_i$

I_3 = identity matrix of order 3.

The hydrodynamic coefficients are usually given in the body's frame. The total external forces are then computed in the ship's frame and so transformed to the $0xy\psi$ system where equation (2.3) is integrated.

2.2. Exciting and Dissipative Forces

In the present section wave, wind and current forces will be discussed under a semi-empirical approach.

2.2.1. Wave exciting forces in a low frequency range

As previously mentioned, a moored vessel excited by waves oscilates about another position than the static equilibrium one, in two distict frequency ranges: the wave spectrum range and near

the eigenfrequencies of the system on the horizontal plane. Both oscilations have the same order of magnitude.

The oscilation in the primary range is caused by forces known as first-order forces since their appearance is related with the solution of the first-order diffraction problem.

The oscilation in the low frequency range however, denotes a non-linear behaviour. As shown firtst by Maruo (1960) and then by Newman, Hsu & Blenkarn and others authors, the appearance of slow-varying forces lies on the second-order solution of the diffraction problem. If considered to second-order, a monochromatic wave causes a constant drift force forcing the ship to move away from its static equilibrium position. Now, considering the existence of wave groups, which can be seen as an amplitude modulation, such drift force will vary with the same frequency of the group, usually about 10^{-2} Hz. Due to its high inertia and low mooring restorance the eigenfrequencies of the moored vessel system, on the horizontal plane, usually lies in such range. So, ressonance may occur, and in spite of the magnitude of second-order forces, vessel oscillations in the low frequency range may be of the same magnitude of first-order oscillations.

Thus, three basic conditions are necessary for slow-drift to occur:

i) narrow band wave spectrum

ii) non-linear diffraction

iii) low restoring force causing low natural frequencies.

The exact solution of the second-order wave force problem may be achieved by solving the non-linear diffraction potential and then integrating the total pressure over the hull:

$$p = -\rho \frac{\partial \phi}{\partial t} - \frac{1}{2} \rho \left[\nabla \phi_1\right]^2 - \rho g z \tag{2.4}$$

where:

$\phi = \phi_1 + \phi_2$

ϕ_1 = first-order potential

ϕ_2 = second-order potential

The total potential ϕ is equated by, correct to second-order:

$$\nabla^2\phi = 0$$

$$\frac{1}{g}\frac{\partial^2\phi}{\partial t^2} + \frac{\partial\phi}{\partial z} = \frac{1}{g}\left[2\,\nabla\phi\,\nabla\left(\frac{\partial\phi}{\partial t}\right) - \frac{1}{g}\frac{\partial\phi}{\partial t}\frac{\partial}{\partial z}\left(\frac{\partial^2\phi}{\partial t^2} + g\frac{\partial\phi}{\partial z}\right)\right] \quad \text{at free surface} \qquad (2.5)$$

$$\frac{\partial\phi}{\partial z} = 0 \quad \text{at bottom}$$

plus a boundary condition at body's surface extended to second-order terms and a radiantion condition as $x \to \infty$.

Obviously, the solution of equation (2.5) is not trivial. This problem is now being worked out at IPT, but have been solved under some restrict conditions, by Newman, Faltinsen, Pinkster, and others authors.

In the present work a semi empirical procedure is used to determine second-order wave forces according to Maruo, Hsu & Blenkarn, Remery & Hermans, and others.

2.2.1.1. Extention of Maruo's Formula

Maruo's equation, for a monochromatic wave, relates the mean drift forces to the squared amplitude of the wave by means of the reflection coeficient.

$$D(\omega) = \frac{1}{2}\rho g\, R^2(\omega)\,\mathbb{A}^2 \qquad (2.6)$$

Hsu & Blenkarn method extends Maruo's equation to irregular waves calculating the second-order forces using something like a convolution integral in time domain:

$$D(t,\ x) = \frac{1}{2}\rho g \int_{-\infty}^{t} F^{-1}\left(R^2(f)\right)\, A^2(t-\tau,\ x)\, d\tau \qquad (2.7)$$

where:

F = Fourier Transform

Neverthless, such procedure limits the study to a given heading angle. Overpassing this limitation the here presented procedure calculates the drift force by means of a integration over the ship's water line.

$$Du(t) = \int_{WL} \vec{f}_2(t,\ s)ds.\vec{u}$$

$$Dv(t) = \int_{WL} \vec{f}_2(t,\ s)ds.\vec{v} \qquad (2.8)$$

$$D\psi(t) = \int_{WL} \vec{f}_2(t,\ s) \times \vec{r}(s)ds.(\vec{u} \times \vec{v})$$

where

s = contour coordinate

$\vec{f}_2(t,\ s)$ = second-order force per unit lenght

$\vec{r}(s)$ = position vector related to ship's C.G.

$\vec{u},\ \vec{v}$ = unit vectors, u and v directions.

Since potential flow is assumed for wave description, $\vec{f}_2(t,\ s)$ acts perpendicularly to the body's surface. Plus, the perturbation on wave potential is considered as an attenuation in wave amplitude at the points positioned in the ship's shadow,

relative to the incident wave.

So,

$$\vec{f}_2(t, s) = \frac{1}{2} \rho g \, C_2(s) \, A^2(t, s) \, (\vec{n}.\vec{m})\vec{n} \qquad (2.9)$$

$$C_2 = \begin{cases} 1 & \vec{n}.\vec{m} < 0 \\ 1 - R^2 & \vec{n}.\vec{m} > 0 \end{cases}$$

where

$\vec{n}$ = normal unit vector at s

$\vec{m}$ = unit vector in the wave propagation direction

$A(t, s)$ = wave profile around the water line

Since slow drift ocurrs only in narrow band wave spectrum, a simplification is assumed

$$R^2(f, \theta) = \bar{R}^2 = \frac{1}{\sigma^2} \int_{-\infty}^{\infty} S(f) \, R^2(f, \theta) df \qquad (2.10)$$

where

$S(f)$ = wave spectrum

σ^2 = wave RMS

θ = heading angle

The coefficient $R^2(f, \theta)$ can be either obtained by theoretical computations or model experiments. In equation (2.9) R^2 corresponds to beam heading, simplifying that expression. Actually, as exemplified by results from Tomonaga & Hatakenaka, for a given frequency, $R^2(\theta)$ can be assumed to vary with $sin^2\theta$, peaking at beam heading.

Completing the evaluation of slow drift wave forces it is necessary to know the wave profile contour on the ship's hull. This is straight foward if, in a given time t, the position of the

ship and the wave train is known in a delimited region.

2.2.1.2. Generation and Propagation of an Irregular Wave Train

Some basic assumptions are made, for a chosen wave spectrum:

- o potential flow
- o unidirectional propagation
- o linear dispersion relationship
- o ergodicity

The wave train propagation problem is solved applying a linear space filter g to an wave profile $\zeta(s, t)$ (Fig. 3)

$$\zeta(s, t + \Delta t) = g(\zeta(s, t)) \qquad (2.11)$$

Due to linear dispersion assumption, g can be posed as a convolution integral:

$$\zeta(s, t + t) = \int_{-\infty}^{\infty} g(r) \, \zeta(s - r, t) dr \qquad (2.12)$$

where $g(r)$ is the impulsive response, i.e., it is the resulting wave train in $t + \Delta t$ for an unit impulse in t.

The Fourier Transform

$$G(k) = \int_{-\infty}^{\infty} g(s) \, e^{-iks} \, ds \qquad (2.13)$$

is the filter transfer function, giving, for each wave number k, the space phaseshift $\phi(k)$, relating time t to $t + \Delta t$. Unitary gain is assured by potential flow assumption.

From linear dispersion relationship it can be shown that:

$$\phi(k) = c(k)\Delta t.k \tag{2.14}$$

where

$c(k)$ = wave celerity

The convolution integral (2.12) is implemented using FFT algorithm

$$\zeta(s,\ t + \Delta t) = F^{-1}(Z(k,\ t).G(k)) \tag{2.12'}$$

where

F = Fourier Transform and

$Z(k,\ t) = F\ (\zeta(s,\ t))$

A wave spectrum realization, computed at a point s_o, by means of a white noise filtering technique (Nunes, D.), works as the process input. The initial wave pattern is obtained by propagation, starting from a null profile, until the lowest celerity component has reached the end of the simulation region.

2.2.2. Current Forces and Viscous Damping Forces

Assuming that current forces vary quadratically with current velocity, they can be evaluated under a similar approach taken in foil theory: lift, drag and yaw moment.

$$\begin{aligned} L_c &= \frac{1}{2}\, C_L(\alpha_c)\rho\ BHV_c^2 \\ D_c &= \frac{1}{2}\, C_D(\alpha_c)\rho\ BHV_c^2 \\ M_c &= \frac{1}{2}\, C_M(\alpha_c)\rho\ LBHV_c^2 \end{aligned} \tag{2.15}$$

where the hydrodynamic coefficients must be experimentally

evaluated. Typical examples are show in figs. 5 to 7.

Notice that no coupled effects between current and wave flow field are considered.

The slow variation of the angle of attack (α_c) supports this quasi-static approach to the problem. So one can use in expressions (2.15):

$$\alpha_c(t) = \alpha_{co} + \psi(t) \tag{2.16a}$$

$$\vec{V}_c(t) = \vec{V}_{co} - \vec{V}_G(t) \tag{2.16b}$$

The dissipative forces due to the motions on the horizontal plane are implicitly incorporated in expression (2.16b). Neverthless, the dissipative moment due to yaw velocity is not yet considered.

Disregarding coupled effects between horizontal velocities and yaw rate, i.e., terms in $\dot{u}_i^n.\dot{\psi}^m$ $(i = 1, 2)$ are negligeable, the viscous damping moment due to yaw rate can be written:

$$M_{\dot{\psi}}^{\cdot} = \frac{-1}{4}\rho\,\dot{\psi}|\dot{\psi}|\ \{\int_L C_D(\xi)\ \xi^2|\xi|\ H(\xi)d\xi + \frac{C_{\dot{\psi}}^{\cdot}}{2}\, L^4\} \tag{2.17}$$

where:

$C_D(\xi)$ = 2 - D double section drag coefficient along ship's lenght

L = ship's lenght

$C_{\dot{\psi}}^{\cdot}(\dot{\psi})$ = moment coefficient taking tip vortices at bow and stern into account

$H(\xi)$ = sectional draft

Notice that a strip theory approach was used, and as mentioned by Faltinsen, the drag coefficients, expected to depend on Reynold's and Keulegan-Carpenter numbers, are not easy to evaluate.

2.2.3. *Wind Forces*

As current effect, wind forces are considered under an empirical approach. Wind forces and moments are evaluated by means of empirical coefficients. Many ways have been proposed to estimate wind effects. Faltinsen divides the sailing area in a finite number of parts and associates to each one a drag coefficient.

Due to its own simplicity the semi-empirical method of A.J.W. Lap was used in the present work. In such model a mean constant wind speed is considered. The wind force and moment are given as a function of angle of attack for conventional ships with aft super-structure .

Basically:

$$F_v(t) = \frac{1}{2} C_v(\alpha_v)\rho_a(S_y.cos^2\alpha v + S_x sen^2\alpha v)V_v^2 \qquad (2.18)$$

where:

$C_v(\alpha_v)$ = wind force coefficient

$\alpha_v = \alpha_v(t)$ = angle of attack

V_v = wind speed

ρ_a = air density

S_x = longitudinal projection of sailing area

S_y = transversal projection of sailing area

Typical curves are shown in figs. 9 to 11. Refer to fig. 8 for variables indentification.

2.3. *Restoring Forces Due to Mooring System*

Assuming that hydrodynamic drag acting upon mooring lines is neglectable and disregarding their own inertia, the restoring forces can be considered as conservative, i.e., depending only on

mooring lines' coordinates.

Once horizontal forces (as a function of coordinates) are already known the total restoring force due to the mooring system can be computed.

Two kinds of mooring lines are considered: single anchor chains and composed lines with an intermediate buoy. Steel or nylon cables are not studied in the present work since elasticity effect must be incorporated to the model. Such study are now under development at IPT.

2.3.1. *Single Anchor Chain Lied on Sea Bottom*

Fig. 12 shows a tipycal scetch of such line. The point where the line touchs the sea bottom is an unknown that must be eliminated.

From classical catenary equation, after some mathematical work, it follows a nondimensional relation between horizontal force at line's tip and horizontal displacement.

$$\xi = f\left(\sqrt{\frac{1 + 2f}{f^2}} - ln\left(\frac{1}{f} + 1 + \sqrt{\frac{1 + 2f}{f^2}}\right)\right) \qquad (2.19)$$

with:

$$\xi = \frac{S - X}{D} \qquad (2.20)$$

$$f = \frac{H}{\mu D}$$

where:

ξ = nondimensional horizontal displacement

S = total chain's length

D = depth

f = nondimensional horizontal force

μ = specific weight of the chain

Expression (2.19) is plotted in fig. 13. f_1 is the dimensionless total force at chain's tip.

2.3.2. Anchor Chains with Fixed Ends

This is the case exampled by fig.14 and corresponds to anchor lines fixed to intermediate buoys.

Refering to fig. 14 and equating the chain static equilibrium, it follows:

$$D = \frac{2H}{\mu} \sinh \frac{\mu x}{2H} \sinh \frac{\mu(x - 2xo)}{2H}$$

$$S = \frac{2H}{\mu} \sinh \frac{x}{2H} \cosh \frac{\mu(x - 2xo)}{2H} \qquad (2.21)$$

and so:

$$\cosh^{-1} \frac{\mu S}{2H \sinh \frac{\mu x}{2H}} = \sinh^{-1} \frac{\mu D}{2H \sinh \frac{\mu x}{2H}} \qquad (2.21a)$$

After some algebric effort:

$$\xi = \frac{1}{f} \sinh^{-1}\left(\frac{1}{f}\right) \qquad (2.22)$$

with:

$$f = \frac{2H}{\mu\sqrt{S^2 - D^2}}$$

$$\xi = \frac{x}{\sqrt{S^2 - D^2}} \qquad (2.23)$$

where:

f = nondimensional horizontal force

ξ = dimensionless horizontal displacement

Fig. 15 shows the graphic of expression (2.22).

2.3.3. Mooring Lines with Intermediate Buoys

Assuming the buoy dynamics as neglectable, equation (2.22) can be applied to each portion of the mooring line (see Fig. 16).

The static equilibrium position of the buoy is computed, at each instant t, by minimizing the function:

$$\phi(\alpha, \beta) = (H_2 - H_1)^2 + (V_2 + V_1 + E)^2 \qquad (2.24)$$

where:

$H_i(\alpha, \beta)$ = horizontal force applied to the buoy by i^{th} portion of the mooring line.

$V_i(\alpha, \beta)$ = vertical force

E = effective buoyance

3. STATIC EQUILIBRIUM POSITION ON THE HORIZONTAL PLANE

The static equilibrium position of the ship on the horizontal plane is solved using minimum potential energy principium applied to the mooring system action.

Each mooring line acts as a nonlinear spring defined by equations (2.19) or (2.22), or by the procedure shown in section 2.3.3., in the case of a intermediate buoy.

The following basic assumptions are made on mooring line forces:

- action on mooring line vertical plane
- depend on coordinates

Since mooring line forces depend only on coordinates, the can be assumed as derivatives of a potential function. So, the total potential energy of the mooring system is the summation of each line contribution.

The problem of potential energy minimization is solved using the conjugate gradient method. For each mooring line, force and potential energy are extracted from equations (2.19) or (2.22)

Such method allows to identify indiferent equilibrium positions, if any, by checking the potential second derivative eingenvalues.

4. SOME TYPICAL RESULTS

A tanker moored to a symmetrical mooring arrangement, composed by four anchor chain lines was chosen to ilustrate the computing procedure (Fig. 17). Table 1 presents the system's particulars.

Figures 19 to 22 show some examples of computed time series.Fig. 18 shows the simplified wave spectrum used for these examples. The spectrum bandwidth was chosen to tuning the second mode eigenfrequency (y direction)

First-order response was computed by inserting a simplified first-order model for surge, sway and yaw modes. However, usual first-order R.S.O. results, based on ship theory method, can be easily introduced.

Figures 19 and 20 correspond to wave excitation at a 45 degrees heading. Figures 21 and 22 correspond to wave and wind excitation at a 45 degrees heading plus a current action at a 270 degrees of incidence. Table 2 shows the environmental conditions.

Notice the large amplitude of motions and mooring line tensions at low-frequencies. The non-linear response characteristic of mooring lines is preserved, leading to larger first-order dynamic forces as low-frequency componentes reaches a maximum.

TABLE 1. SYSTEM PARTICULARS

TANKER	
displacement	12.282 t
length b.p.	148 m
beam	18,9 m
draft	6,2 m
sailing area	200 m^2/550 m^2
MOORING SYSTEM	
Anchor Chains	
length	200 m
linear density	0,8 KN/m
yeld force	1.410 KN
depth	50 m

TABLE 2. SIMULATED ENVIRONMENTAL CONDITIONS

WAVE	
significant height	1.5 m
up-zero crossing period	9.5 sec
heading	45º
WIND	
intensity	5 m/s
heading	45º
CURRENT	
intensity	0,25 m/s
heading	270º

5. CONCLUDING REMARKS

The present model covers comprehensively the different aspects involved in the moored vessel problem. It allows to consider the mooring line non-linear characteristics and to simulate the system behaviour under general environmental conditions. First and second-order effects due to wave action are tanken into account leading to helpful informations for mooring system design and operation.

Neverthless, the semi-empirical nature of the model presumes an accurate estimation of coefficients for each specific case. As a consequence of such inherent uncertanties the simulation program must be considered as a design tool, able to compare the behaviour of different mooring configurations but not yet accurate enough to yield exact magnitudes of forces and motions.

Further studies, including the exact solution of second--order wave diffraction problem at different depths and considering elastic mooring lines, as ropes or wire-cables, are essential to the development of more accurate and comprehensive models.

The current and wind action models may be improved, noticing however that probably its empirical nature will be not eliminated.

REFERENCES

1. FALTINSEN, O.M. & LOKEN, A.F. Slow drift oscillation of a ship in irregular waves. MODELING, IDENTIFICATION AND CONTROL, 1980. V. 1, nº 4, 185-213.

2. HSU F. H. & BLENKARN, K.A. Analysis of peak mooring force caused by slow vessel drift oscillation in ramdon seas. In: OFFSHORE TECHNOLOGY CONFERENCE, 2º, Houston, Apr. 22-24, 1970. V.1, p. 135-146.

3. MARUO, H. The drift of a body floating on waves. Journal of Ship Research, 4(3):1 - Dec. 1960.

4. MOTORA, S. On the measurement of added mass and added moment of inertia of ships in steering motion. In: SYMPOSIUM on SHIP MANEUVERABILITY, 1º, Washington, D.C., May 24-25, 1980. Washington, D.C., DTMB, 1960. p. 241-273. (David Taylor Model Basin - Report 1461).

5. NEWMAN, J.N. Marine Hydrodynamics. Cambridge. M.I.T., 1978. 402p.

6. NEWMAN, J.N. Second-order, slowly-varying forces on vessels in irregular waves. In: INTERNATIONAL SYMPOSIUM on the DINAMICS of MARINE VEHICLES and STRUCTURES in WAVES, London, Apr. 1-5, 1974. London, IME, 1975. p. 182-186.

7. NUNES, DANTON. Random wave generation by linear digital filtering of Gaussian white noise. In: SECOND INTERNATIONAL CONGRESS OF THE IMAEM, Trieste, Sep. 21-26, 1981.

8. PESCE, CELSO P. Medições em escala real das tensões agentes nas amarras de um navio cisterna. São Paulo, IPT/DINAV, 1981. 29p. (Trab. apres. ao 7º Congresso Panamericano de Engenharia, Transportes Marítimos e Engenharia Portuária, Viña del Mar, out. 1981).

9. PINKSTER, J.A. & VAN OORTEMERSEN, G. Computation of the first and second order wave forces on oscillating bodies in regular waves. s.n.t.

10. REMERY, G.F.M. & HERMANS, A.J. The slow drift oscillations of a moored object in ramdon seas. In: OFFSHORE TECHNOLOGY CONFERENCE, 3º, Houston, Apr. 19-21, 1971. V.2, p. 829-838.

11. TOMONAGA, Y. & HATAKENAKA, K. Measurements of the drifting force and moment on floating type offshore structures in waves. Transactions of the West Japan Society of Naval Architects, (59): 33-42, Mar- 1980.

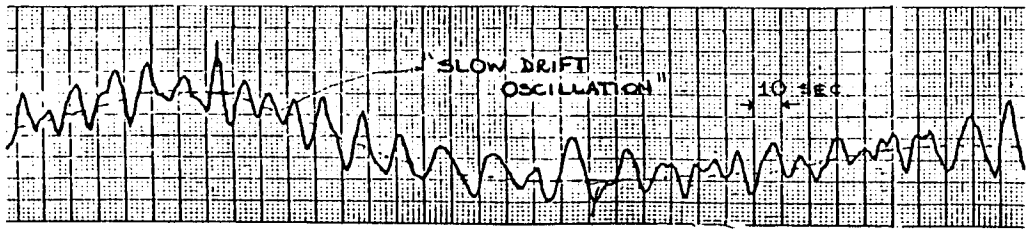

Fig. 1 - Full Scale Measurement of Mooring Forces

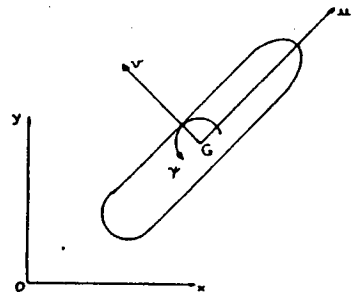

Fig. 2 - Reference Frames

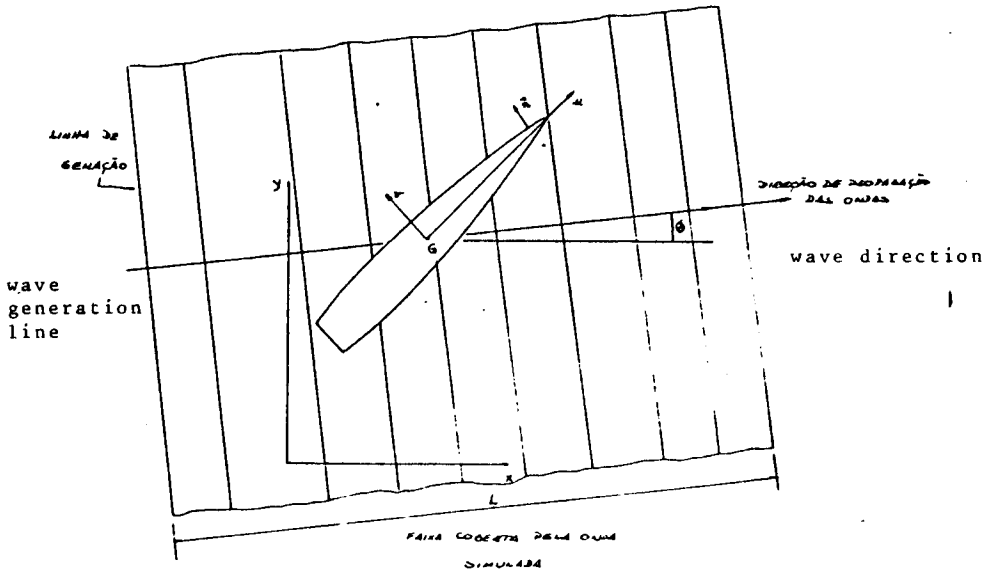

Fig. 3 - Wave Train Propagation Scheme

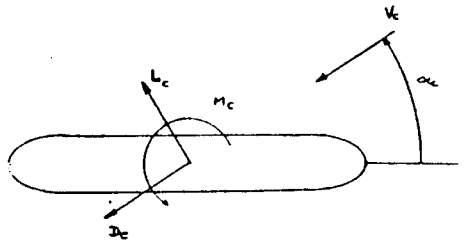

Fig. 4 - Current Force

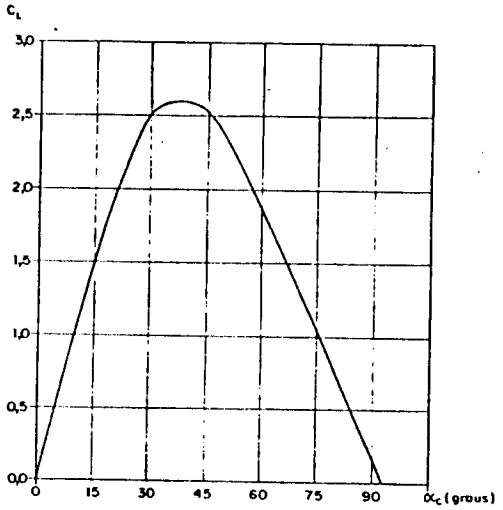

Fig. 5 - Lift Coefficient Due to Current Action X Heading Angle

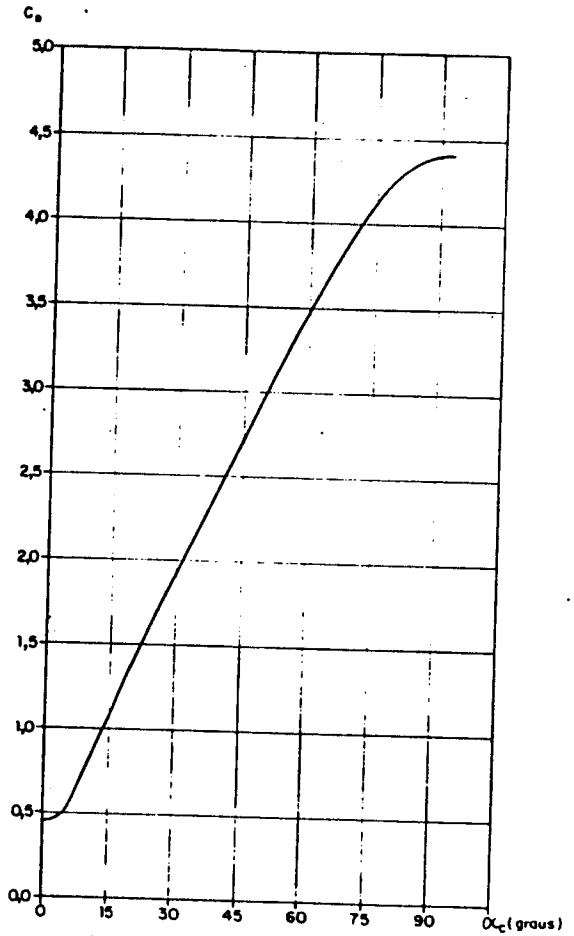

Fig. 6 - Drag Coefficient Due to Current Action X Heading Angle

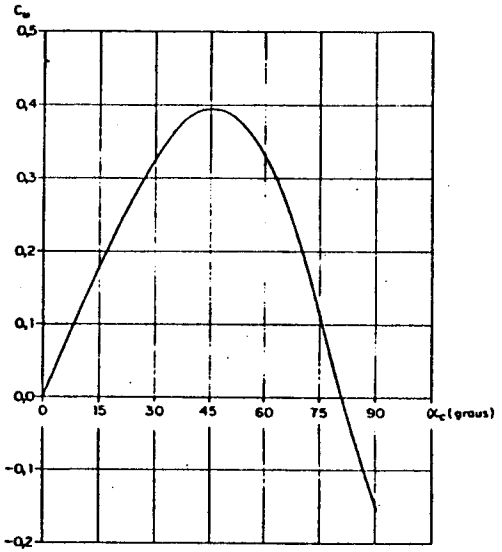

Fig. 7 - Moment Coefficient Due to Current Action X Heading Angle

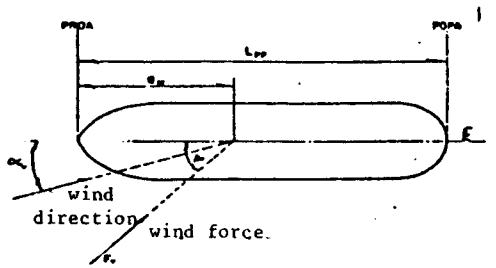

Fig. 8 - Wind Force Scheme

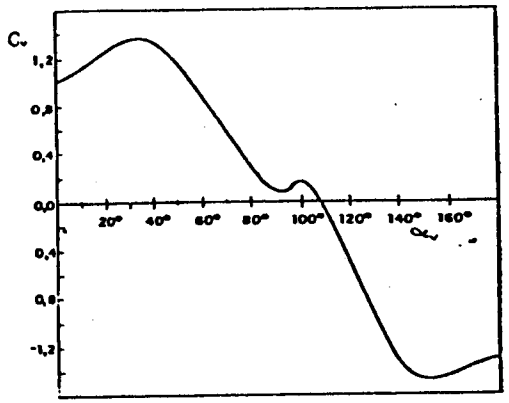

Fig. 9 - Wind Coefficient (C_v) X Heading Angle (α_v)

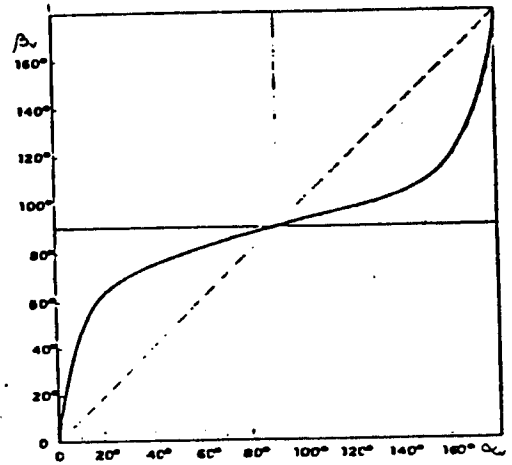

Fig. 10 - Wind Force Direction (β_v) X Heading Angle (α_v)

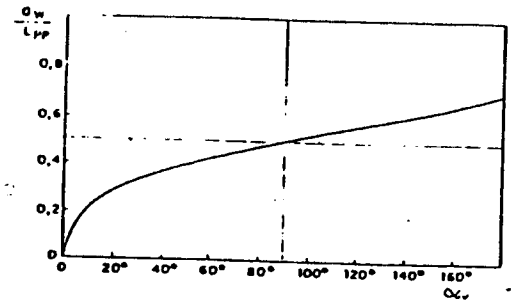

Fig. 11 - Wind Pressure Center Coefficient ($\frac{a_w}{L_{pp}}$) X Heading Angle (α_v)

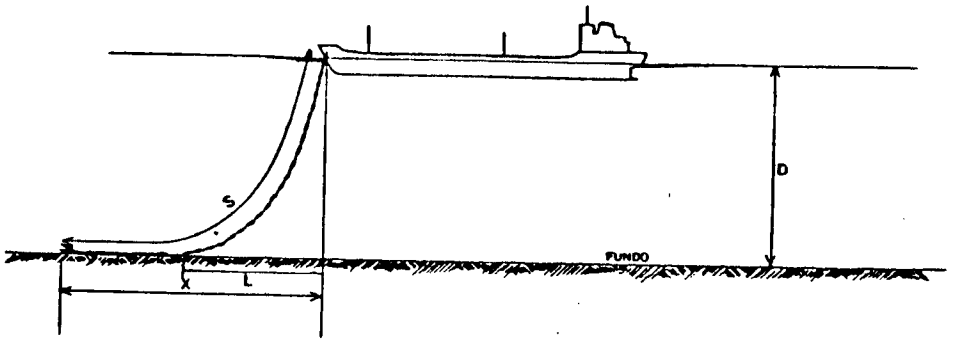

Fig. 12 - Single Chain Mooring Line

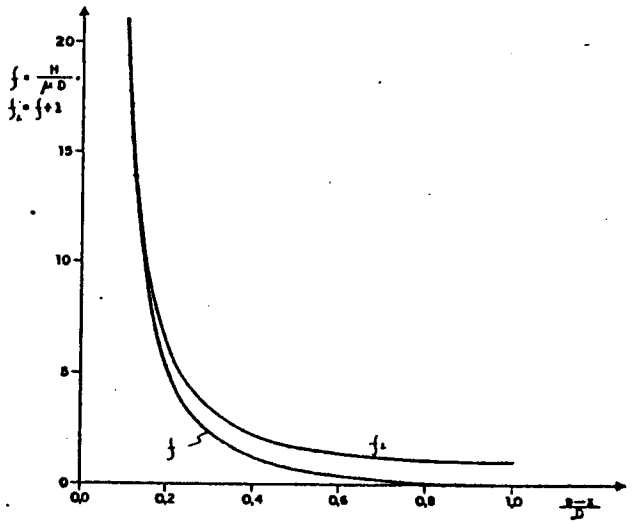

Fig. 13 - Single Chain Mooring Line Dimensionless Horizontal Force Coefficient (f) X Horizontal Displacement

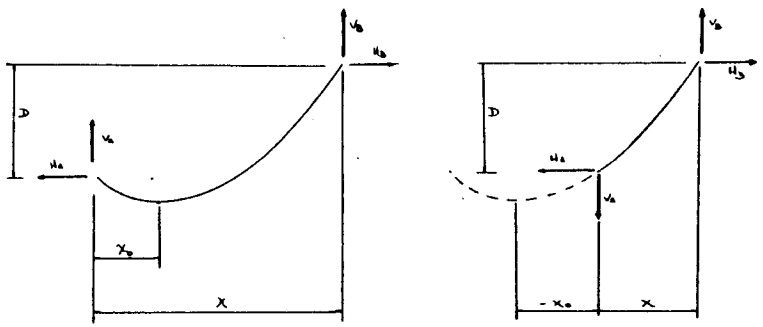

Fig. 14 - Partial Cattenary Lines

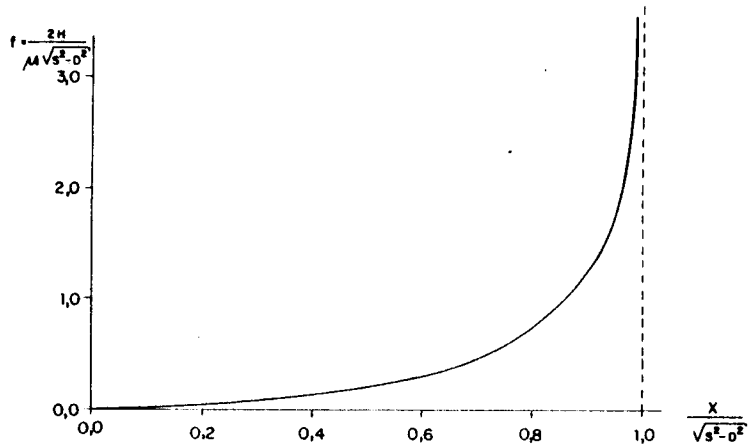

Fig. 15 - Single Partial Mooring Line Dimensionless Horizontal Force Coefficient (f) X Horizontal Displacement

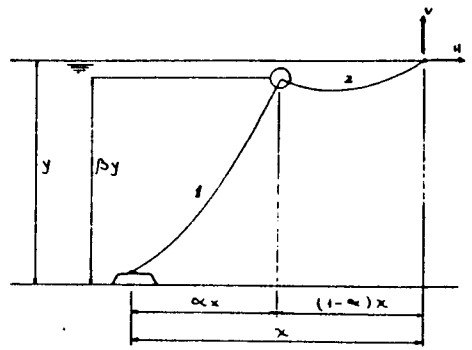

Fig. 16 - Composed Mooring Line By Means of an Intermediate Buoy

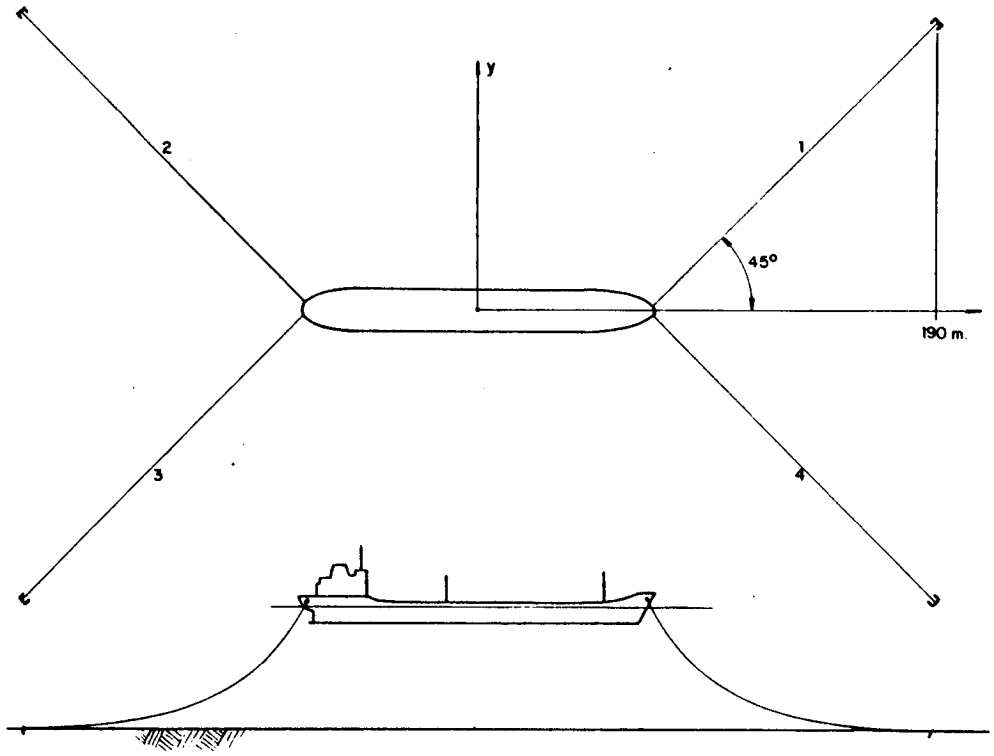

Fig. 17 - Moored Tanker

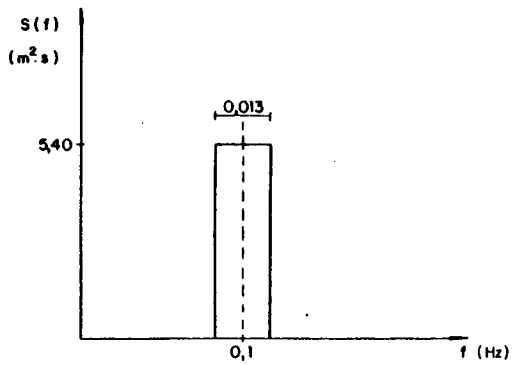

Fig. 18 - Simplified Wave Spectrum Used for Dynamic Simulation of Moored Tanker

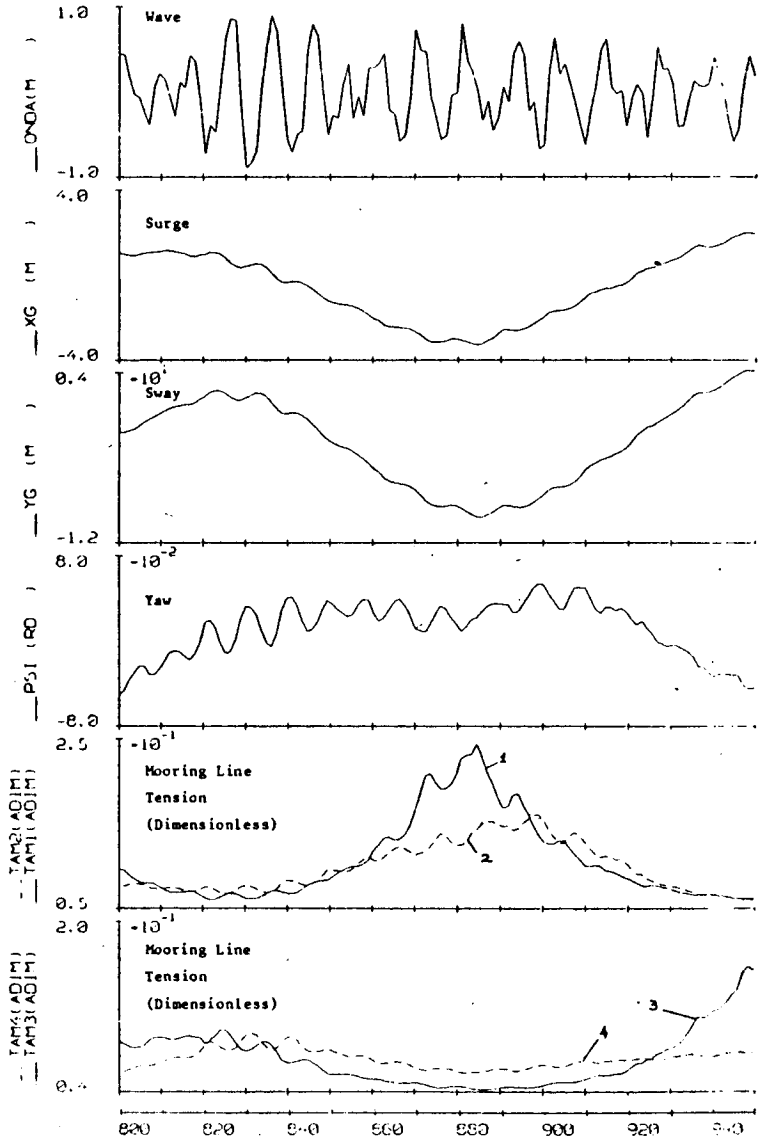

Fig. 19 - Dynamic Simulation of a Moored Tanker Wave at 45º Bow Heading

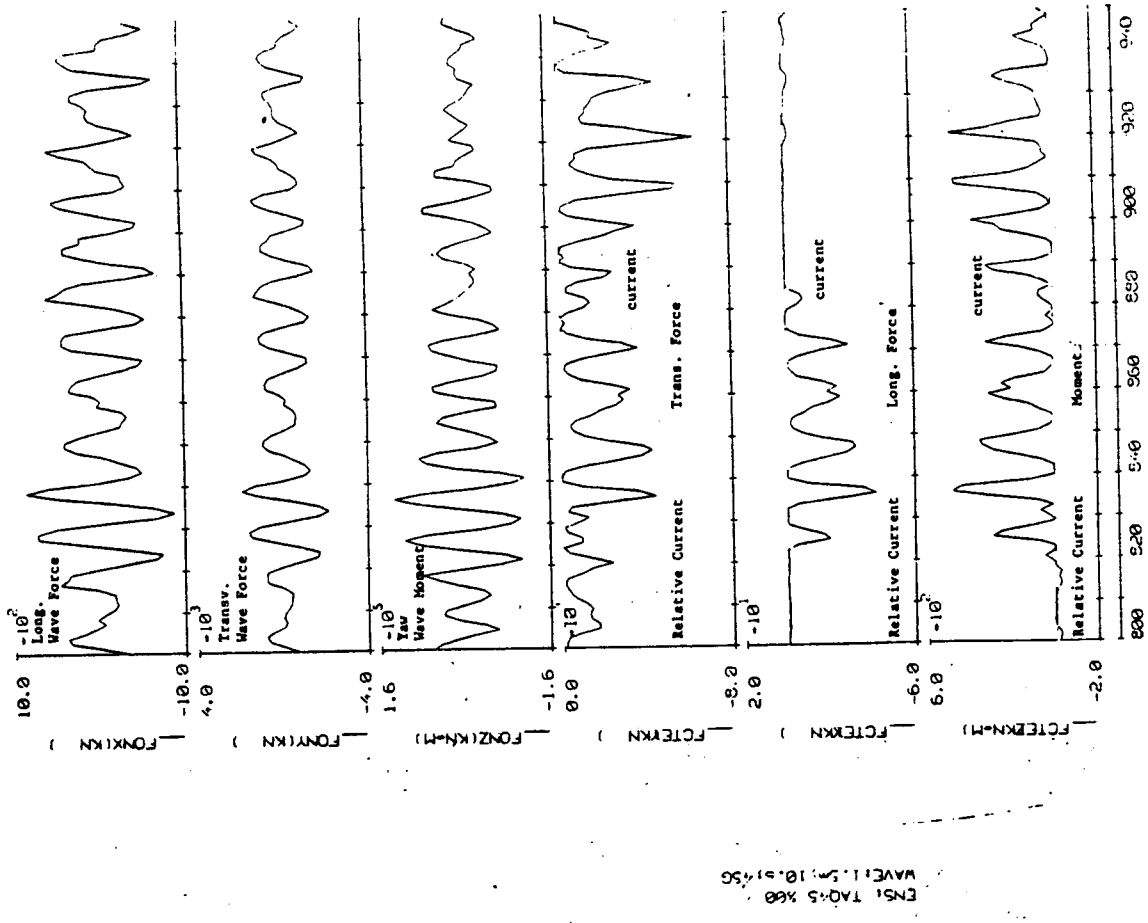

Fig. 20 - Dynamic Simulation of a Moored Tanker
Wave at 45º Bow Heading

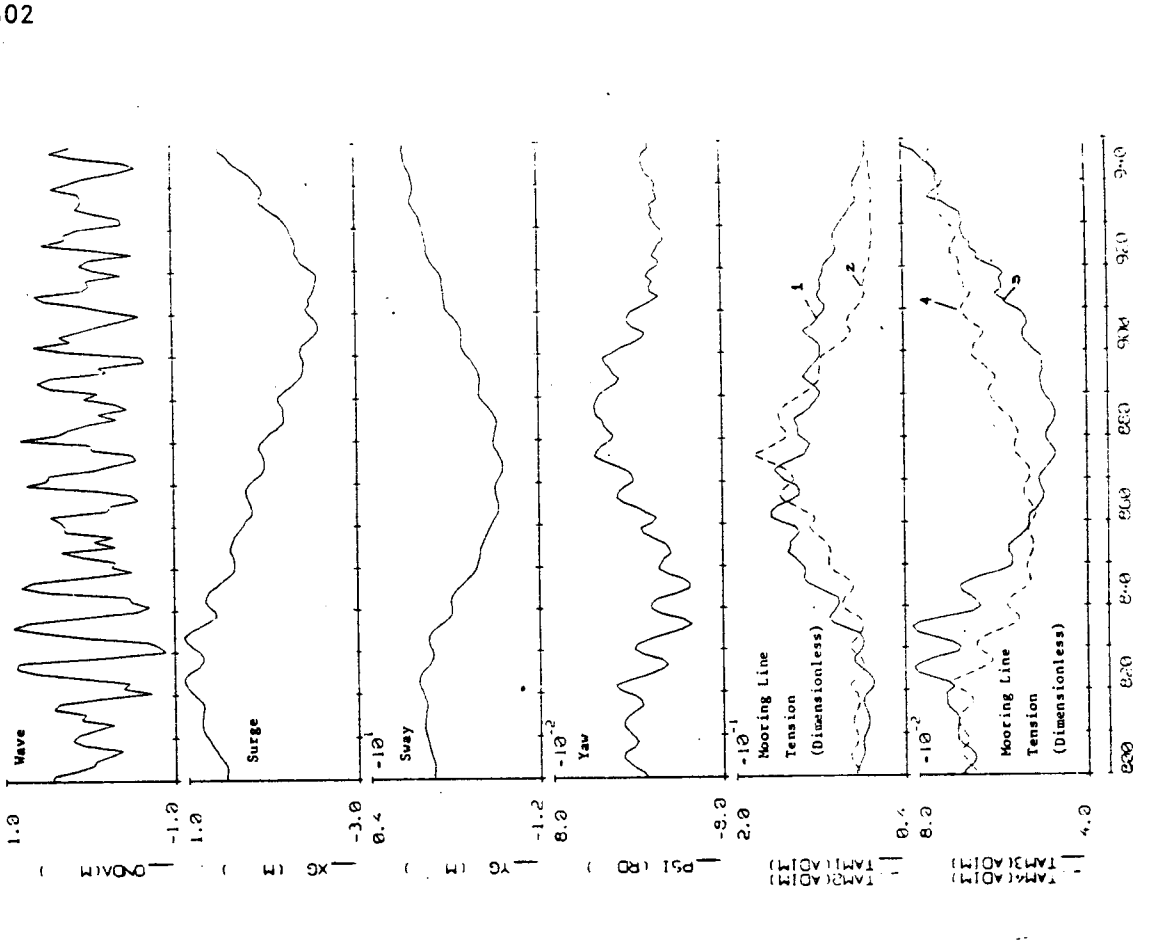

Fig. 21 - Dynamic Simulation of a Moored Tanker, Wave, Wind at 45º; Current at 270º Heading

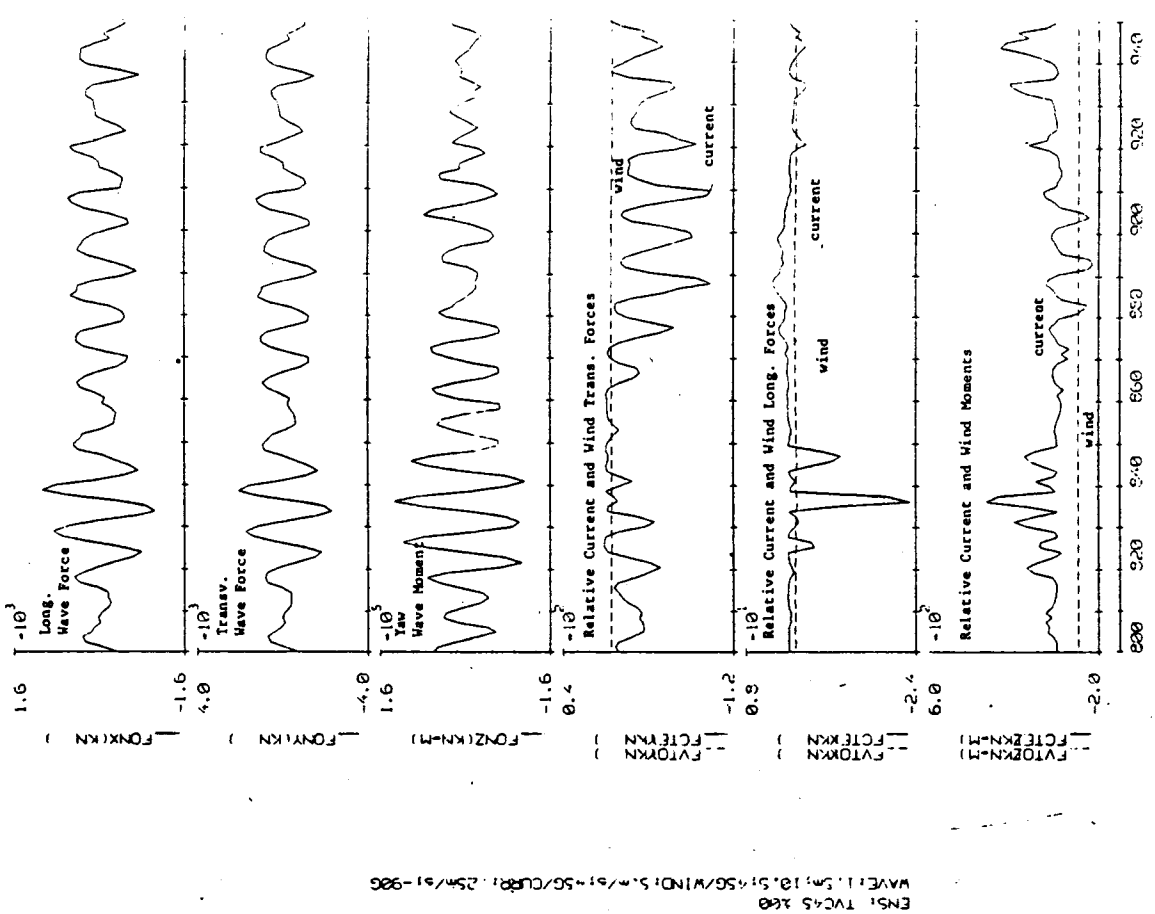

Fig. 22 - Dynamic Simulation of a Moored Tanker, Wave, Wind at 45°; Current at 270° Heading